Heterogeneity in social and epidemiological factors determines the risk of measles outbreaks

Paolo Bosetti[a,b,1], Piero Poletti[a,1,2], Massimo Stella[a], Bruno Lepri[a], Stefano Merler[a,3], and Manlio De Domenico[a,3]

[a]Center for Information and Communications Technology, Fondazione Bruno Kessler, 38123 Povo (Trento), Italy; and [b]Mathematical Modelling of Infectious Diseases Unit, Institut Pasteur, UMR2000, CNRS, 75015 Paris, France

Edited by Roy M. Anderson, Imperial College London, London, UK, and accepted by Editorial Board Member Simon A. Levin October 1, 2020 (received for review November 29, 2019)

Political and environmental factors—e.g., regional conflicts and global warming—increase large-scale migrations, posing extraordinary societal challenges to policymakers of destination countries. A common concern is that such a massive arrival of people—often from a country with a disrupted healthcare system—can increase the risk of vaccine-preventable disease outbreaks like measles. We analyze human flows of 3.5 million (M) Syrian refugees in Turkey inferred from massive mobile-phone data to verify this concern. We use multilayer modeling of interdependent social and epidemic dynamics to demonstrate that the risk of disease reemergence in Turkey, the main host country, can be dramatically reduced by 75 to 90% when the mixing of Turkish and Syrian populations is high. Our results suggest that maximizing the dispersal of refugees in the recipient population contributes to impede the spread of sustained measles epidemics, rather than favoring it. Targeted vaccination campaigns and policies enhancing social integration of refugees are the most effective strategies to reduce epidemic risks for all citizens.

multiplex networks | human mobility | infectious diseases | population dynamics

Human migration represents a complex phenomenon influencing in several interconnected ways the economy, the healthcare, and the social cohesion of whole countries (1–7). However, it is only recently that the availability of massive datasets opened to new advancements in modeling and understanding such complexity (8–16), addressing the urgent need for effective, large-scale intervention policies toward managing the consequences of massive migration flows (5).

Here, we focus our attention on Turkey, a country facing a humanitarian emergency of unprecedented levels (17). In the last decade, more than 3.5 million (M) Syrians, displaced by the war, have sought refuge in Turkey. The arrival of a huge amount of people with different economic, health, and living conditions, and from a country where the healthcare system has been almost completely disrupted, may raise serious concerns about the risks of the Turkish health system being overburdened.

Turkish infectious-disease specialists are concerned that the crisis of Syrian refugees may impose serious risks to Turkey by bringing back infectious diseases previously eliminated or in the process of being eliminated (18, 19). According to the latest reports from the World Health Organization (WHO) and the United Nations Children's Fund (UNICEF) (20), immunization coverage in Syria dropped from more than 80% before the war to a worrying 41% in 2015 for the most basic vaccines, resulting in millions of unvaccinated children. Direct consequences of this alarming situation are a high risk of epidemic outbreaks [e.g., evidence for polio (21) and measles (22–24) has been reported] and a potential increase of mortality due to diseases which could be prevented with vaccines (25). Countries, such as Turkey, Lebanon, and Jordan, hosting a great concentration of Syrians perceive the lack of an appropriate immunization coverage as a potential risk of epidemic outbreaks for the local population (18).

The aim of this study is to investigate the risk of observing widespread measles epidemics in Turkey and how this risk is affected by the level of mixing between refugees and the local populations. After the influx of Syrian refugees, an increase of measles cases has been observed (24), and two measles outbreaks in 2013 and 2018 have been reported (24, 26, 27). In order to reduce the risk of vaccine-preventable diseases, the Ministry of Health of Turkey—in collaboration with UNICEF—conducted several vaccination campaigns between 2013 and 2014. Syrian children living in and out of temporary shelters have been vaccinated free of charge and are now included in the Turkish National Childhood Vaccination Program. Refugees have been receptive to vaccination, and recent estimates suggest that a 95% vaccine uptake was reached in the temporary shelters. However, in this country, more than 90% of the Syrian population lives in communities where immunity levels might be significantly lower, and seeking vaccination services remains a problem because of high mobility and lack of knowledge about refugee health centers (23).

The contribution of our work is twofold. On the one hand, we quantify the epidemic risks associated with measles in Turkey and how appropriate policies devised to enhance social integration between refugees and local populations may significantly reduce the risk of observing widespread epidemics. On the other hand, we highlight crucial epidemiological and socio-demographic components shaping these risks, identifying

Significance

The recent increase in large-scale migration trends generates several concerns about public health in destination countries, especially in the presence of massive incoming human flows from countries with a disrupted healthcare system. Here, we analyze the flow of 3.5 M Syrian refugees toward Turkey to quantify the risk of measles outbreaks. Our results suggest that heterogeneity in immunity, population distribution, and human-mobility flows is mostly responsible for such a risk: In fact, adequate policies of social integration and vaccine campaigns provide the most effective strategies to reduce measles disease risks for both migrant and hosting populations.

Author contributions: P.B., P.P., B.L., S.M., and M.D.D. designed research; P.B., P.P., M.S., B.L., S.M., and M.D.D. performed research; P.B., P.P., and M.S. analyzed data; and P.B., P.P., M.S., B.L., S.M., and M.D.D. wrote the paper.

The authors declare no competing interest.

This article is a PNAS Direct Submission. R.M.A. is a Guest Editor invited by the Editorial Board.

[1]P.B. and P.P. contributed equally to this work.

[2]To whom correspondence may be addressed. Email: poletti@fbk.eu.

[3]S.M. and M.D.D. contributed equally to this work.

This article contains supporting information online at https://www.pnas.org/lookup/suppl/doi:10.1073/pnas.1920986117/-/DCSupplemental.

First published November 17, 2020.

high-risk areas in the country that should be prioritized by public health interventions aimed at reducing current immunity gaps.

Results

The risk of measles reemergence in Turkey was analyzed by using a multilayer transmission model, explicitly taking into account potential infectious contacts occurring between individuals moving across the country. In the model, Turkey was divided into 1,021 patches corresponding to Turkish prefectures, which are spatial subunits of provinces and of the largest cities, reflecting administrative districts and metropolitan municipalities. The absolute number of Syrian and Turkish individuals in each prefecture and moving between patches was inferred from available mobile-phone data (28), following an approach similar to one used in previous studies (29–33). Measles immunity across different Turkish provinces for the two populations was estimated by combining epidemiological records available from different sources (4, 20, 24, 26, 27, 34) and taking into account possible geographical heterogeneity in measles-vaccine uptake (13–15). Measles transmission was modeled by considering a tunable parameter that accounted for a variety of scenarios on how much refugees interact with Turkish citizens, ranging from full segregation to full integration.

A schematic representation of the model is shown in Fig. 1, along with spatial mobility patterns inferred by the analysis of call detailed records (CDRs) associated with the usage of mobile phones in the country. An overview of the model structure and of the proposed methodological approach is reported in *Materials and Methods*. Technical details can be found in *SI Appendix*.

Measles Immunity Levels in Turkey. To overcome the lack of serological data, we inferred the fraction of susceptible individuals in the two populations by analyzing the epidemic growth rate of cases reported for Syria in 2017, the spatial heterogeneity in the proportion of children vaccinated in Turkey between 2006 and 2016, and the age distribution of cases reported during recent measles outbreaks (2013–2018).

The dynamics of infectious diseases are strongly determined by the infection-transmission potential, which can be measured through the basic reproduction number (R_0), defined as the average number of secondary infections generated by a typical case in a fully susceptible population (35–40). When considering diseases with preexisting levels of immunity (e.g., childhood diseases like measles), a measure of the actual transmission potential is provided by the effective reproduction number (R_e) (36, 40, 41).

We found that R_e associated with a measles epidemic that recently occurred in Syria was 1.27 (95% CI 1.19 to 1.37). Consequently, we estimated that the percentage of susceptible individuals in this country at the beginning of 2017 was 8.62% (95% CI 6.96 to 10.71%), while the percentage of susceptible individuals among Syrian refugees in Turkey was estimated to be 9.5% (95% CI 7.7 to 11.8%; Fig. 2). The spatial displacement of Syrian refugees in Turkey as inferred by CDRs (Fig. 1) clearly suggests that the current amount of refugees among different provinces is neither homogeneous over space nor proportional to local population sizes (Fig. 3).

Estimates obtained for Turkish citizens suggest that the percentage of susceptible Turkish citizens is lower than 5% in 92% of the Turkish prefectures. At the national level, only 2.3% of Turkish people might be currently susceptible to measles infection. However, this percentage ranges between 1.78% and 10.0% across prefectures, and worryingly high levels of susceptibility among Turkish citizens were found in some provinces

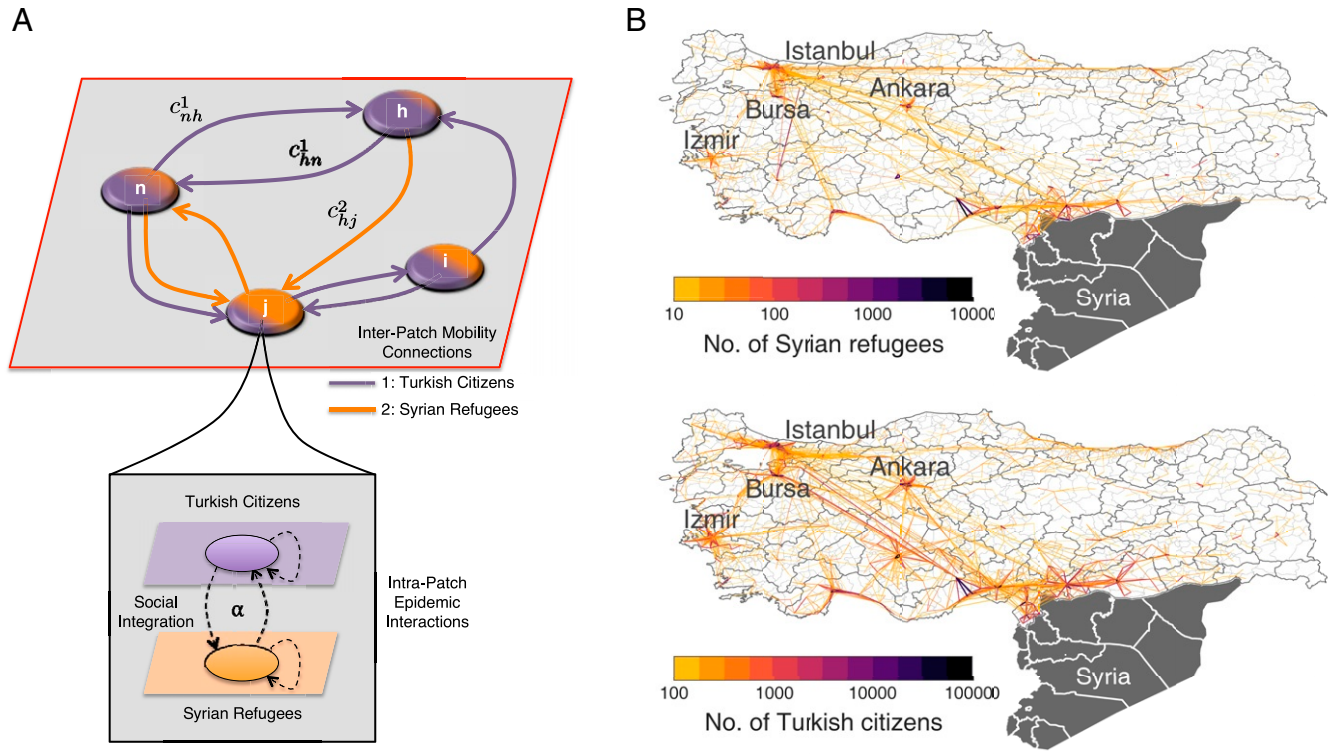

Fig. 1. Model structure and human mobility. (*A*) Schematic illustration of the model considered in this work. Each prefecture of Turkey is considered as a node of a metapopulation network of geographic patches. Two populations, namely, Turkish and Syrians, are encoded by different colors and move between patches following the inferred interpatch mobility pathways. Turkish and Syrian populations encode two different layers of a multilayer system (31–33), where social dynamics and epidemics spreading happen simultaneously. (*B*) Mobility of Syrian refugees (*Upper*) and Turkish citizens (*Lower*) between the prefectures of Turkey as inferred from CDRs. Different colors are used to indicate the number of individuals moving from a prefecture to another.

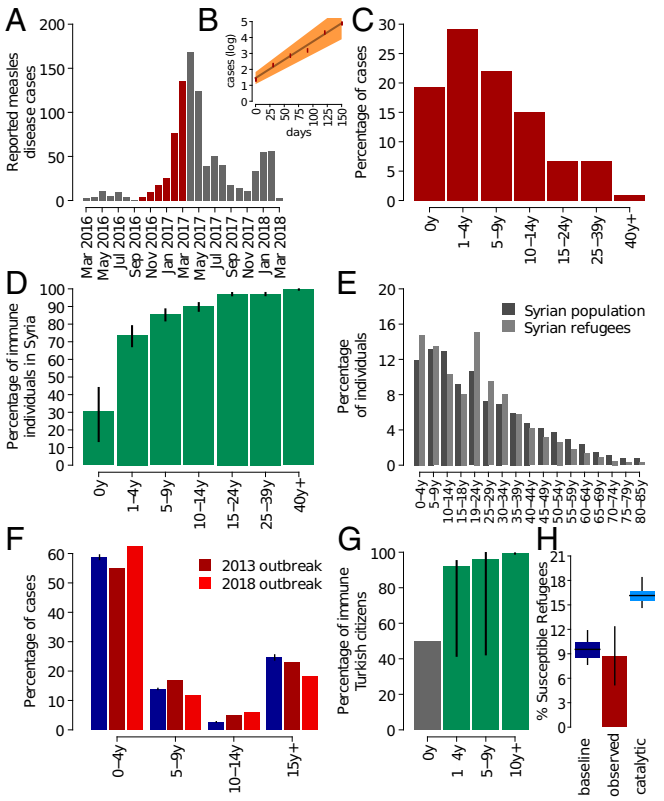

Fig. 2. Measles immunity levels. (*A*) Reported number of measles disease cases over time, during the 2016–2018 measles epidemics in Syria, as recently reported by the WHO (27); red bars correspond to data points used to derive the R_e as a function of the exponential growth rate of the observed epidemic. (*B*) Obtained fit of the epidemic exponential growth between September 2016 and February 2017 in Syria: The red solid line represents the mean estimate; the orange shaded area represents 95% CI. (*C*) Observed distribution of measles cases across different ages during the 2016–2018 measles epidemics in Syria, as recently reported by the WHO (27). (*D*) Model estimates of the age-specific immunity profile in Syria at the beginning of 2018: Green bars represents mean values; vertical black lines represent 95% CI. (*E*) Observed age distribution of Syrian refugees in Turkey (light gray) (42) compared with the population age distribution in Syria (dark gray). (*F*) Estimated (blue) and observed (red) distribution of measles cases across different ages during the 2013 and 2018 measles epidemics in Turkey. (*G*) Model estimates of the age-specific immunity profile in Turkey at the beginning of 2018. The gray bar represents the level of measles immunity in infants, here assumed to be 50%, as a consequence of maternal antibodies. Vertical bars in the age bands 1 to 4 y and 5 to 9 y show the variability (minimum and maximum) across different Turkish provinces in the immunity level of these age segments. The vertical bar shown for individuals older than 10 y of age represents the 95% CI of the immunity level in this age segment, as obtained by fitting the model on the age distributions of cases shown in *F*. (*H*) Estimated percentage of susceptible individuals among Syrian refugees in Turkey. Blue and light blue boxplots represent the immunity estimates obtained with the baseline model and by using the catalytic method, respectively. The red bar shows the observed immunity level among Syrian refugees reported in ref. 43 in a refugee cohort in Germany in 2015. Black lines represent the 95% CI.

in the southeast of the country, close to the borders with Georgia, Armenia, Iran, Iraq, and Syria (Fig. 3). These regions should be considered at risk for measles epidemics, regardless of the presence and the level of integration of Syrian refugees.

For endemic diseases like measles, a rough estimate of the proportion p of immune population (either due to vaccination or natural infection) required to prevent large outbreaks can be inferred by using the widely accepted equation $p = 1 - 1/R_0$ (38–40, 44). In our simulations, we explored values of R_0 ranging from 12 to 18, which are typical values of R_0 estimated for measles in other countries (38–40). For these values of R_0, areas with a proportion of susceptible individuals larger than 5 to 8% are potentially at risk for sustained local transmissions.

Obtained results suggest that, nowadays, in Turkey, 270,000 to 410,000 out of 3.5 M Syrian refugees and about 1.8 M out of 80 M Turkish people are measles-susceptible. The resulting fraction of susceptible population across different Turkish prefectures (*SI Appendix*) suggests that provinces located on the border with Syria are those at a major risk of local measles transmission because of low local immunity levels among Turkish citizens and of a high concentration of susceptible refugees in the resident population.

In the extreme and rather unrealistic case of no mixing between the two populations, the infection would separately spread within each population, registering few cases in the highly immune Turkish population and causing way larger outbreaks in the highly susceptible population of Syrian refugees.

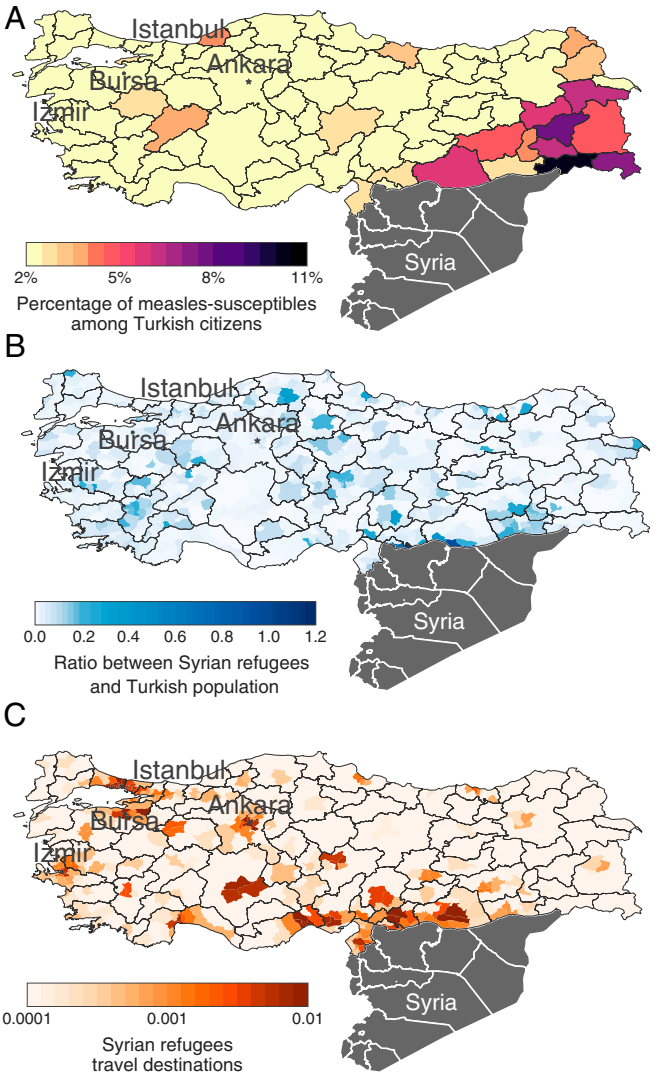

Fig. 3. Risk factors. (*A*) Percentage of measles-susceptible Turkish citizens as estimated across different prefectures (34). (*B*) Ratio between Syrian refugees and Turkish population—i.e., $N_k^{(R)}/N_k^{(T)}$—as inferred from CDRs. (*C*) Proportion of traveling refugees visiting the different Turkish prefectures.

Social Integration and Measles-Epidemic Risks in Turkey. We simulated measles transmission in Turkey, under different hypothetical scenarios on the level of mixing of refugees with local populations, taking into account mobility patterns inferred from CDRs. Our results show that the risk of observing large epidemics and the consequent number of cases increase with the basic reproduction number and the proportion of susceptible among the refugees and decrease with the increasing level of social integration between Syrian and Turkish citizens (Fig. 4 and *SI Appendix*).

High levels of mixing between refugees and Turkish citizens have the potential of preventing the spread of measles in many prefectures and can reduce by 75 to 90% the overall number of measles cases of potential epidemics (Fig. 4–6). In fact, when refugees mix well with the Turkish, potentially infectious contacts would more probably occur with Turkish immune individuals, who represent about 90% of people currently living in Turkey. On the contrary, in the case of low mixing between the two populations, measles transmission is sustained by the lack of adequate immunity levels among refugees. In particular, we found that if only 20% of Syrian contacts occur with Turkish citizens, the risk of observing sustained transmission in the country is large for any value of R_0 larger than 15, but also for lower values of R_0 (e.g., $R_0 = 12$) if the proportion of refugees susceptible is 9.5% or more (*SI Appendix*). In this case, measles epidemics could produce nonnegligible spillover of cases among local residents as well, causing thousands of Turkish cases all over the country (Fig. 4). Regardless of the level of integration considered, significant spillover of cases among Turkish citizens is expected to mainly arise when the onset of measles epidemics occurs on the eastern border with Syria and Iraq, where local measles transmission is possible, even in the absence of Syrian refugees, as a consequence of local low immunity among Turkish citizens.

We found that if 9.5% of refugees are measles-susceptible, the probability of observing an epidemic that causes at least 20 cases among Syrian refugees and Turkish citizens decreases from 100% (high segregation) to less than 10% (high integration), and, in the case of outbreak, when refugees mix well with Turkish citizens, the expected overall number of cases becomes no larger than a few hundred (*SI Appendix*).

Spatial Diffusion of Potential Epidemics. We analyzed simulations' results to identify the potential spatiotemporal spread of measles epidemics in Turkey and highlight how high segregation levels are also expected to promote the spatial invasion of the epidemic across the whole country. Figs. 5 and 6 show the impact of measles epidemics randomly started in one of 100 prefectures more at risk for local transmission, under a worst-case scenario, where $R_0 = 18$ and the percentage of susceptible Syrian refugees is 11.8%. In this case, when more than 90% of Syrian contacts occur within the Syrian population, measles epidemics are expected to affect more than 300 of 1,021 prefectures of Turkey (Fig. 6*A*). On the contrary, for the majority of considered epidemiological scenarios, if more than 70% of contacts of refugees occur with Turkish people, as a consequence of refugees' good integration with Turkish citizens, measles epidemics are expected to remain geographically bounded in less than 10 prefectures of the country (Fig. 6 and *SI Appendix*). Apparently, beyond local levels of immunity, frequent destinations for both Turkish and Syrian people represent areas that are most at risk for being affected by large epidemics (Figs. 1, 3*C*, and 6).

Our results suggest that the level of social integration between refugees and the Turkish population can strongly affect the spatiotemporal spread of potential epidemics. Fig. 6 *E*–*H* show for each prefecture the expected cumulative measles incidence over time for different levels of social integration under the worst-case scenario. Obtained estimates indicate that, in the case of full segregation, 43% of Turkish prefectures are expected to experience more than 10 measles cases after 30 weeks since the beginning of an epidemic. Such percentage decreases to 16%, 4%, and 1% when refugee contacts with Turkish citizens increase to 20%, 40%, and 60%, respectively. Interestingly, in the case of full segregation, prefectures where cases of infections are registered at earlier stages are mainly located in regions associated with the four largest cities of Turkey (62%; Fig. 6*E*). In contrast, when 60% of refugees' contacts occur with Turkish citizens, a remarkable fraction of prefectures that would be affected in the

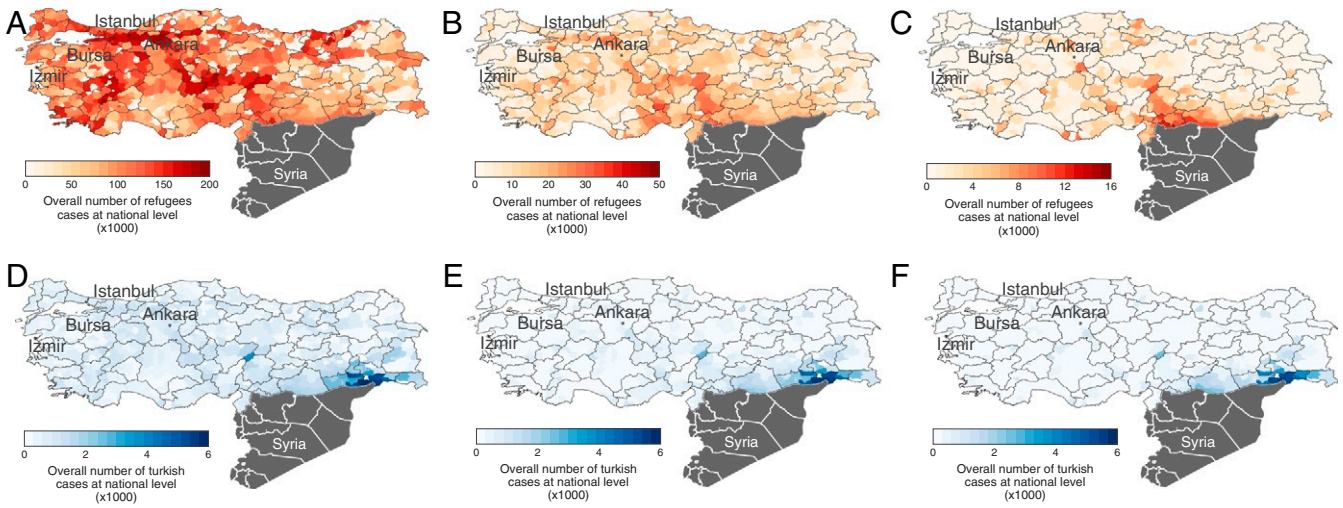

Fig. 4. The potential of widespread measles epidemics. (*A*) Cumulative number of cases among refugees at the national level as expected by considering scenarios where the measles epidemics start from different patches by assuming 20% of Syrian contacts with Turkish citizens, $R_0 = 18$ and that the percentage of susceptible refugees is 11.8%. For each patch, the color encodes the estimated incidence in the total population due to epidemics starting in that prefecture: This choice allows one to appreciate how each geographic area can potentially affect the whole country. (*B*) As in *A*, but for 40% of Syrian contacts with Turkish citizens. (*C*) As in *B*, but for 60% of Syrian contacts with Turkish citizens. (*D*) As in *A*, but considering cases among Turkish citizens. (*E*) As in *D*, but for 40% of Syrian contacts with Turkish citizens. (*F*) As in *D*, but for 60% of Syrian contacts with Turkish citizens.

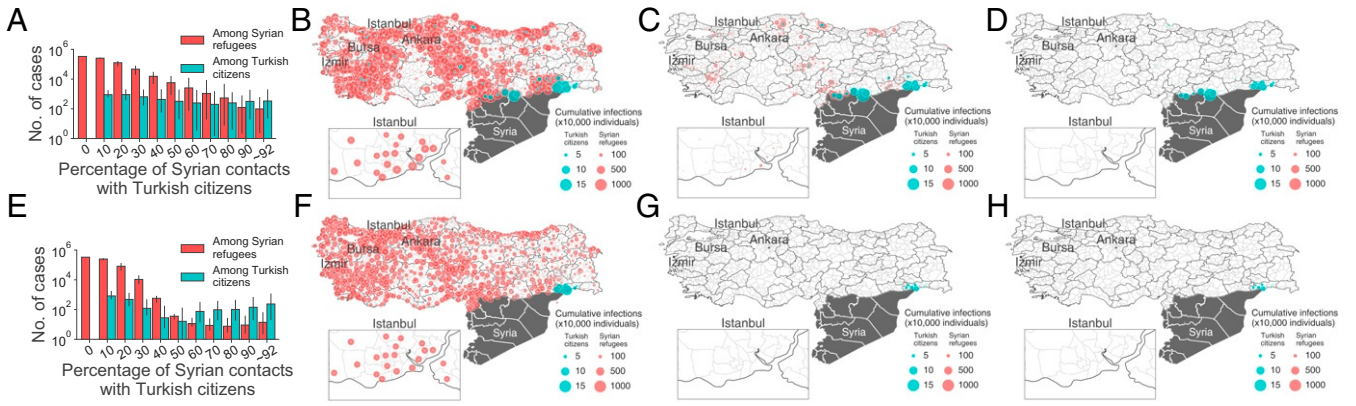

Fig. 5. The potential burden of measles epidemics. (*A*) Cumulative infections considering epidemics that exceed 20 cases in the entire population, as obtained in a worst-case scenario where $R_0 = 18$, the percentage of susceptible refugees is set at 11.8%, and epidemic onset randomly occurs in one of the 100 most at-risk prefectures in Turkey. Bars represent the average number of infections occurring among Syrian refugees (red) and Turkish citizens (blue) for the model projections as a function of the mixing parameter; black lines represent 95% CI. (*B*) Estimated cumulative infections in the case of 20% of Syrian contacts with Turkish citizens. Bubble size is proportional to the average number of measles cases in the Turkish prefectures per 10,000 individuals. *B*, *Inset* displays the Istanbul prefectures. (*C*) As in *B*, but for 40% of Syrian contacts with Turkish citizens. (*D*) As in *B*, but for 60% of Syrian contacts with Turkish citizens. (*E*) As in *A*, but as obtained when refugees are assumed to be geographically dispersed in each patch proportionally to the amount of local Turkish residents. (*F*) As in *B*, but as obtained when refugees are assumed to be geographically dispersed in each patch proportionally to the amount of local Turkish residents. (*G*) As in *F*, but for 40% of Syrian contacts with Turkish citizens. (*H*) As in *F*, but for 60% of Syrian contacts with Turkish citizens.

early phase of a measles epidemic are close to the Syrian border (Fig. 6*H*).

Risk Areas and Risk Factors. We combined different model results to identify geographical areas at major risk of measles outbreaks, highlighting risk factors that may determine the onset of large epidemics. Results presented so far suggest that, for any considered scenario, areas at major risk of measles epidemics are represented by prefectures located on the border with Syria, where the susceptible fraction among Turkish citizens is large (Fig. 3*A*) and the percentage of Syrian refugees in the population is high (Fig. 3*B*).

When the mixing of refugees with local population is low (e.g., due to segregation), additional high-risk areas both for Turkish citizens and Syrian people are represented by prefectures where the overall fraction of susceptible population is high, either due to a massive presence of Syrians (e.g., close to Izmir; Fig. 3*B* and *SI Appendix*) or due to low immunity among the Turkish citizens (e.g., northeast of Ankara; Fig. 3*A* and *SI Appendix*).

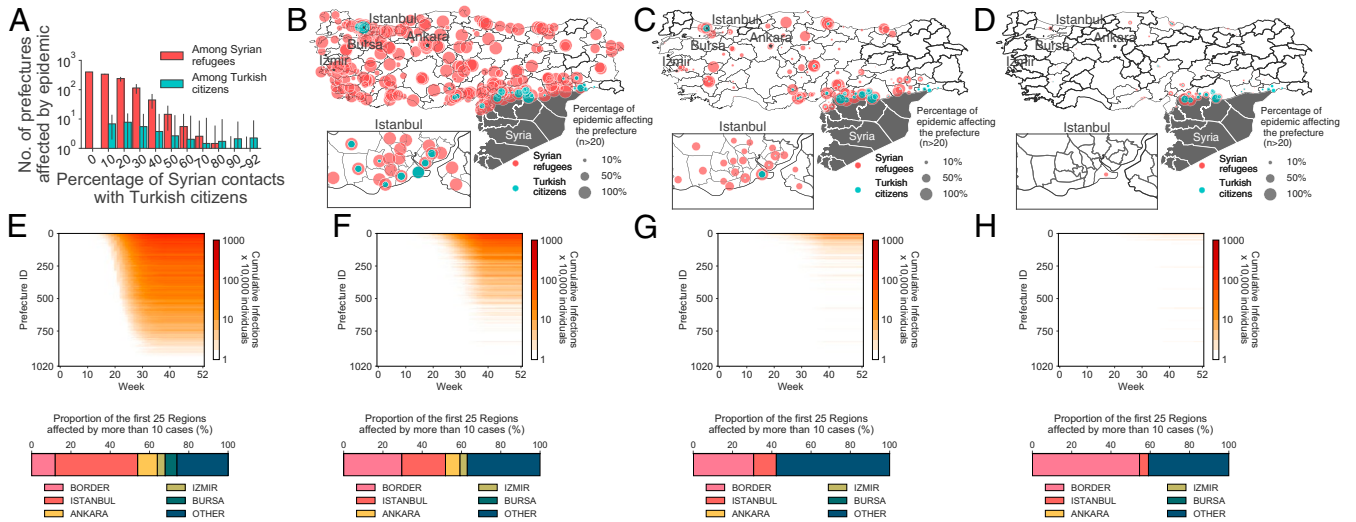

Fig. 6. Spatiotemporal spread of potential epidemics. (*A*) Estimated number of prefectures affected by the epidemic as a function of the mixing parameter in the worst-case scenario, where $R_0 = 18$, the percentage of susceptible refugees is set at 11.8%, and epidemic onset randomly occurs in one of the 100 most at-risk prefectures in Turkey. Bars represent the average number of prefectures exceeding 20 cases among Syrian refugees (red) and Turkish citizens (blue); black lines indicate the 95% CI. (*B*) Percentage of the simulated epidemic that exceeds 20 cases per prefecture in the case of 20% of Syrian contacts with Turkish citizens. Red and blue bubbles refer to Syrian refugees and Turkish citizens, respectively. (*C*) As in *B*, but for 40% of Syrian contacts with Turkish citizens. (*D*) As in *B*, but for 60% of Syrian contacts with Turkish citizens. (*E*, *Upper*) Relative incidence over time, considering both the populations per prefecture in the case of total segregation. Prefectures are ranked in decreasing order at week 30. (*E*, *Lower*) Proportion of region affected in the initial phase of the epidemic, considering the first 25 prefectures affected by more than 10 cases. Border refers to the Hatay, Kilis, Gaziantep, Sanliurfa, Mardin, and Sirnak regions. (*F*) As in *E* in the case of 20% of Syrian contacts with Turkish citizens. (*G*) As in *E* in the case of 40% of Syrian contacts with Turkish citizens. (*H*) As in *E* in the case of 60% of Syrian contacts with Turkish citizens.

However, our results also suggest that—even under a hypothetical scenario of high integration—the percentage of Syrian refugees in the population appears as a possibly relevant risk factor influencing both the expected number of cases among Syrians and the amount of spillover of cases among the Turkish citizens (e.g., Figs. 3*B* and 5). We, therefore, simulated measles epidemics under an illustrative scenario by considering $R_0 = 18$ and 11.8% susceptible refugees, but assuming that refugees are displaced in the Turkish territory proportionally to the Turkish residents. For any level of social integration, obtained results (Fig. 5 *E*–*H*) show that, in this case, the risk of observing measles epidemics in Turkey and the potential spillover of cases among Turkish citizens are significantly reduced with respect to outcomes obtained when the actual spatial distribution of refugees in Turkey is considered (Fig. 5).

Discussion

Measles remains the major vaccine-preventable disease threat both for Syrian refugees and local citizens in Turkey (23). The widely accepted critical immunity threshold for measles elimination is 95% of immune individuals (38–40, 44). According to our estimates, as a consequence of the suboptimal vaccination during the ongoing civil war, Syrian refugees hosted in Turkey display a considerably large fraction of individuals that are susceptible to measles (about 90% of immune individuals, though highly uncertain). Although critically low immunity levels were also detected among Turkish citizens living on the border with Syria, the level of protection of the Turkish population against the disease is nearly optimal in 90% of prefectures.

The strong difference in the immunity levels to measles among the two populations may have deep repercussions on society's perception toward the movement of Syrians within Turkey. As is common in Western countries hosting considerable amounts of migrants (45), Turkish citizens might perceive the lower immunization coverage of Syrian refugees as a potential threat to national welfare and health. This perception might be even worsened by the staggering numbers of Syrian refugees registered in Turkey, 3.5 M in 2018 (28, 45). This well-documented negative perception (46, 47) may trigger segregation mechanisms aimed at reducing as much as possible interactions and contacts between Syrian refugees and Turkish citizens.

The carried-out analysis provides compelling evidence that social segregation of refugees does not hamper, but, rather, boosts potential outbreaks of measles.

The main result of the current study is the quantitative evidence that high levels of mixing between Syrian refugees and Turkish citizens can be highly beneficial in drastically reducing the potential spatial spread of measles and the incidence of measles cases both in the refugees and in the host population. This is due to the fact that the high immunization coverage of Turkish citizens can shield Syrian refugees from getting exposed to the infection, and this reduces potential sources of infection, in a virtuous cycle reminiscent of herd immunity (15, 25, 48). Provided that a full homogeneous mixing of refugees and citizens could prove to be impracticable or rather difficult to achieve, policies aimed at reducing social segregation would dramatically reduce current epidemiological risks in the country. As most of susceptible individuals in the country are expected to be younger than 10 y of age (Fig. 2), promoting integration at school among the youngest generations may be particularly effective in reducing the chances of observing sustained transmission of highly infectious diseases such as measles.

From a geographic perspective, immunization campaigns targeting areas characterized by a large amount of refugees with respect to the Turkish population, as is the case of many prefectures close to the Syrian border, can prevent the onset of widespread epidemics. Our analysis also confirmed that metropolitan areas play a pivotal role in spreading the disease over time. These areas are mainly prefectures of Istanbul and Ankara and, unsurprisingly, also include many areas adjacent to the national borders of Turkey with Syria. It is in these areas that the efforts for reducing social segregation should be strategically focused. Finally, our results show that a more spatially homogeneous displacement of refugees in the Turkish population would critically reduce measles risks in the country. Although the number of Syrian refugees in Turkey is fairly stable since 2018, future migration flows have the potential to dramatically change the epidemic risks across different regions.

These modeling results pose some practical challenges for the future. Indeed, as recently reported by the Organisation for Economic Co-Operation and Development (49), integration of migrants and refugees in the host population is a difficult task. National governments generally designed dispersal mechanisms to avoid concentrations of migrants. At the same time, the geographic dispersal of migrants across host countries depends on a number of different factors, such as the presence of existing communities from their country of origin or available work and educational opportunities. Migrants, refugees, and asylum-seekers are themselves highly diverse groups of people and communities, characterized by different cultural backgrounds and with different reasons for migrating, as well as different levels of skills and work experience. All these factors can shape how localities can offer integration services and may create inequalities in terms of the opportunities available to the refugees or prevent effective social integration with local populations. Unfortunately, recent reviews of urban-regeneration projects highlighted an important process of social segregation of minorities and non-Turkish ethnicity particularly strong in large cities such as Istanbul (46).

The performed analysis has several limitations that should be considered in interpreting the results. Estimates of immunity levels in Syrian refugees and in Turkish citizens should be considered cautiously, as no recent serological surveys are available for the two populations. In the model, different immunity levels were inferred from the analysis of available data on measles outbreaks that occurred in Syria and Turkey between 2013 and 2018 (24, 26, 27) and vaccine-uptake records made available by the Demographic Health Survey from Turkey (34) and the WHO (20). Although field measurements, performed through a serological study on the Syrian refugee population in Germany, are compatible with our estimates (Fig. 2), we performed a sensitivity analysis on the robustness of model results, where the proportion of susceptible refugees in Turkey was estimated by a catalytic approach (37, 50, 51). Model estimates obtained in the sensitivity analysis were quantitatively different from those obtained with our baseline approach, but they confirmed the main results on the risk of measles epidemics and the role played by social integration in decreasing measles-infection risks in Turkey (*SI Appendix*).

No data on mixing patterns (e.g., by age) are available for either Syrian refugees or Turkish citizens. Consequently, the model neglects potential differences in measles transmissibility by age of individuals and potential differences in measles transmissibility for Syrian refugees and Turkish citizens (e.g., induced by different numbers of overall contacts). In our model, contact rates of individuals are the same, regardless of their subpopulation, and do not depend on the heterogeneity of the census across different areas. This hypothesis automatically sets that increasing social integration does not alter the number of contacts made by individuals, which may not be the case in reality. However, evidence emerged so far from contact survey studies suggests that there is no difference between the total number or duration of contacts between urban and rural participants (52, 53). Hence, it is fairly reasonable to assume that the overall number

of contacts experienced by an individual is not affected by the human density characterizing the place where the individual lives or by changes in individuals' acquaintance generated by social integration of different communities. The assumption of age independence of contact rate represents a limitation of this study, which does not consider that children, who are the most susceptible, have a higher number of contacts in the population (52–54). Also, we used a single age-independent parameter to model social integration. Therefore, a possible underestimation of the volume of contacts of the children could be partially compensated by their higher chance of integrating. This may be the case of schools, where children usually experience the majority of their contacts (52–54) and where, at the same time, integration has to be favored. Consequently, it is possible that a marked reduction in the attack rate or epidemic risk would require less effort in promoting social integration between local citizens and refugees, as this is eased by certain settings.

Finally, CDR data used in the proposed analysis are associated with just a fraction of the population and do not contain age-specific information of the users. The absence of any age information, together with the fact that children might not own a mobile phone, prevents us from building more complex models with an age-dependent mobility component. In particular, in our model, we assumed that the same mobility patterns characterize individuals of different ages. Although children might be separated by their parents and may be less likely to possess a mobile phone of their own, it is reasonable to assume that most of the children would be accompanied by adults (either their parents or not). Even if CDR data may not perfectly reflect real movements across all of the prefectures, they provide valuable evidence of human mobility in the country that can be used to identify the potential spatiotemporal spread of an epidemic.

Conclusion

The carried-out analysis represents an attempt to quantify the risk of measles reemergence in Turkey and provides striking evidence that social integration of refugees within the Turkish population and maximizing the dispersal of refugees in the country might be effective countermeasures to reduce the chance of observing widespread measles epidemics in Turkey. Public health interventions aimed at increasing measles immunity should prioritize vaccination of Syrian refugees (23) on the national borders of Turkey with Syria and reduce immunity gaps characterizing Turkish citizens in the southeast of the country.

Materials and Methods

Immunity Levels in the Two Populations and Epidemic Risks. Estimates of the immunity level among refugees were obtained by inferring the age-specific fraction of susceptible individuals in Syria during a recent measles epidemic from the growth rate and age distribution of cases reported in 2017 (27) and accounting for the age distribution of Syrian refugees in Turkey (42) (Fig. 2). Specifically, we estimated the effective reproduction number R_e from the growth rate observed on the weekly number of cases reported during the 2017 epidemic in Syria by assuming a uniformly distributed generation time ($T_g \sim U(9, 15)$) (55, 56). Estimates of R_e were used to derive the fraction of susceptible individuals in Syria S_0 at the beginning of 2017, using three values of R_0: 12, 15, and 18 (38–40). Estimates of S_0 were combined with both the age distribution of cases during the epidemic and the age structure of the population to estimate the age-specific immunity profile of the Syrian population. In particular, we assumed that the age distribution of susceptible individuals in Syria should reflect the age distribution of measles cases reported during recent outbreaks that occurred in the country. The rationale behind this assumption was that individuals who were either vaccinated or naturally infected before an observed epidemic could not have been infected during that epidemic. Finally, by using the age distribution of the Syrian refugees in Turkey, we estimated the total number of susceptible individuals among them.

Measles immunity levels among Turkish citizens were estimated for each province by combining available records on the geographical heterogeneity of measles-vaccine uptake observed in Demographic and Health Surveys data from Turkey (13–15, 34) with the most recent WHO estimates of vaccination coverage at the national level (20) and with the age distribution of measles cases recorded during the 2013 and 2018 outbreaks (26, 27). Specifically, we: 1) assumed that the proportion of immune children younger than 10 y of age reflected the fraction of immunized individuals among birth cohorts between 2006 and 2016 through first- and second-dose routine vaccination programs (20); and 2) estimated the susceptible fraction of individuals older than 10 y by assuming that the age distribution of susceptible individuals at the national level should reflect the age distribution of measles cases reported during recent outbreaks that occurred in the country (24, 26). Although natural infection might have contributed to increased immunity in individuals less than 10 y old, less than 9,000 cases were observed in Turkey from 2007 to 2017. We therefore assumed that the impact of measles circulation on the immunity level in this age band is negligible. More details are reported in *SI Appendix*.

Transmission Model. To model measles transmission in Turkey and the mobility of Turkish and Syrian refugees, we assumed two populations of individuals, namely, population T of size $N^{(T)}$ and population R of size $N^{(R)}$, living in a territory consisting of L distinct geographically patches (i.e., Turkish prefectures) accounting for $N_k^{(T)}$ and $N_k^{(R)}$ individuals, $k = 1, \ldots, L$ with $\sum_{k=1}^{L} N_k^{(T)} = N^{(T)}$ and $\sum_{k=1}^{L} N_k^{(R)} = N^{(R)}$.

The formulation of the force of infection for the two populations encodes how the interplay between the level of mixing of refugees with local populations and their mobility patterns shapes the spatial spread of simulated epidemics (12, 16, 29, 57–61).

Let us indicate by $c_{ki}^{(p)}$ ($p \in T, R$) the elements of a matrix $\mathbf{C}^{(p)}$ encoding the number of people belonging to population p traveling from patch k to patch i, and with α the fraction of Syrian contacts with Turkish citizens. The force of infection for each population in the i-th patch depends on the contribution of all patches in the country:

$$\lambda_i^{(T)}(\alpha, \mathbf{C}^{(T)}, \mathbf{C}^{(R)}) = \beta_T \sum_{k=1}^{L} \left[\underbrace{c_{ki}^{(T)} \frac{I_k^{(T)}}{N_k^{(T)}}}_{\text{Endogenous}} + \underbrace{\alpha c_{ki}^{(R)} \frac{I_k^{(R)}}{N_k^{(R)}}}_{\text{Exogenous}} \right], \quad [1]$$

$$\lambda_i^{(R)}(\alpha, \mathbf{C}^{(T)}, \mathbf{C}^{(R)}) = \beta_R \sum_{k=1}^{L} \left[\underbrace{\alpha c_{ki}^{(T)} \frac{I_k^{(T)}}{N_k^{(T)}}}_{\text{Exogenous}} + \underbrace{c_{ki}^{(R)} \frac{I_k^{(R)}}{N_k^{(R)}}}_{\text{Endogenous}} \right], \quad [2]$$

where $\beta_p = \beta / P_i^{(p)}(\alpha, c)$ is the transmission rate for population p and $P_i^{(p)}(\alpha, c)$ is an appropriate normalization factor (such that all individuals have the same number of contacts, regardless of geography and citizenship; see *SI Appendix* for further details). Each contribution consists of an endogenous term, accounting for the infectivity due to individuals from the same population, and an exogenous term, accounting for the infectivity due to the other population. The possible levels of mixing between refugees and Turkish citizens are modeled by considering a tunable parameter (i.e., α).

The absolute number of individuals moving between patches was inferred from available CDRs, as in refs. 28–30, and rescaled to adequately represent the volumes corresponding to 80 M Turkish individuals and 3.5 M Syrian refugees. The original dataset consisted of 1 y of call records of Turk Telekom (TT), one of the major communication companies in Turkey, collected from January 1 to December 31, 2017. In 2017, TT accounted for 24.7% of market share in the country, including customers among Syrian refugees (28). Analyzed data comprised calls of 992,457 customers of TT, 184,949 of which were classified as refugees and 807,508 as Turkish citizens. The geographical reference of individual calls was used to derive mobility patterns at the spatial scale of Turkish prefectures. Additional details on the TT dataset are provided in *SI Appendix*, while for a full and comprehensive description of the dataset, we refer to ref. 28. Finally, details on our model assumptions are provided in *SI Appendix*.

Data Availability. The mobile-phone data were received for the Data for Refugees Turkey Challenge (D4R) and were open for analysis only to the registered and accepted teams, including ours. Other datasets we used are publicly available. To protect the privacy of the users (Turkish citizens and Syrian refugees), mobile-phone data cannot be shared by the authors. The findings presented in our work can be replicated by using publicly

available datasets and by asking for data access for relevant mobile-phone datasets from TT. Interested researchers should apply for data access by contacting TT at d4r@turktelekom.com.tr. Code and data required to reproduce the main findings of the paper are publicly available on Zenodo at https://zenodo.org/record/4227667 (62) and upon request to TT.

ACKNOWLEDGMENTS. We thank TT and the other collaborators (e.g., Bogazici University, Tubitak, Data-Pop Alliance, UNICEF, the United Nations High Commissioner for Refugees, the International Organization for Migration, etc.) of the D4R challenge, as well as the Organization Committee and the Project Evaluation Committee.

1. I. Abubakar *et al.*, The UCL–Lancet commission on migration and health: The health of a world on the move. *Lancet* **392**, 2606–2654 (2018).
2. L. A. Sjaastad, The costs and returns of human migration. *J. Political Econ.* **70**, 80–93 (1962).
3. P. H. Cheong, R. Edwards, H. Goulbourne, J. Solomos, Immigration, social cohesion and social capital: A critical review. *Crit. Soc. Policy* **27**, 24–49 (2007).
4. C. Zimmerman, L. Kiss, M. Hossain, Migration and health: A framework for 21st century policy-making. *PLoS Med.* **8**, e1001034 (2011).
5. S. Castles, H. De Haas, M. J. Miller, *The Age of Migration: International Population Movements in the Modern World* (Macmillan International Higher Education, New York, NY, 2013).
6. B. Rechel, P. Mladovsky, D. Ingleby, J. P. Mackenbach, M. McKee, Migration and health in an increasingly diverse Europe. *Lancet* **381**, 1235–1245 (2013).
7. B. K. Blitz, A. d'Angelo, E. Kofman, N. Montagna, Health challenges in refugee reception: Dateline Europe 2016. *Int. J. Environ. Res. Public Health* **14**, 1484 (2017).
8. X. Lu, L. Bengtsson, P. Holme, Predictability of population displacement after the 2010 Haiti earthquake. *Proc. Natl. Acad. Sci. U.S.A.* **109**, 1576–1581 (2012).
9. P. Deville *et al.*, Dynamic population mapping using mobile phone data. *Proc. Natl. Acad. Sci. U.S.A.* **111**, 15888–15893 (2014).
10. V. D. Blondel, A. Decuyper, G. Krings, A survey of results on mobile phone datasets analysis. *EPJ Data Sci.* **4**, 10 (2015).
11. X. Lu *et al.*, Unveiling hidden migration and mobility patterns in climate stressed regions: A longitudinal study of six million anonymous mobile phone users in Bangladesh. *Global Environ. Change* **38**, 1–7 (2016).
12. Q. Zhang *et al.*, Spread of Zika virus in the Americas. *Proc. Natl. Acad. Sci. U.S.A.* **114**, E4334–E4343 (2017).
13. S. Takahashi, C. J. E. Metcalf, M. J. Ferrari, A. J. Tatem, J. Lessler, The geography of measles vaccination in the African Great Lakes region. *Nat. Commun.* **8**, 15585 (2017).
14. C. E. Utazi *et al.*, Mapping vaccination coverage to explore the effects of delivery mechanisms and inform vaccination strategies. *Nat. Commun.* **10**, 1633 (2019).
15. S. A. Truelove *et al.*, Characterizing the impact of spatial clustering of susceptibility for measles elimination. *Vaccine* **37**, 732–741 (2019).
16. M. C. González, C. H. Hidalgo, A. L. Barabási, Understanding individual human mobility. *Nature* **453**, 779–782 (2008).
17. United Nations High Commissioner for Refugees, "UNHCR, 2017 Annual Report (3RP) Regional refugee & resilience plan 2017-2018" (Tech. Rep., United Nations High Commissioner for Refugees, Geneva, Switzerland, 2018).
18. S. Hargreaves, Concerns in Turkey about infections from refugees. *Lancet Infect. Dis.* **16**, 782–783 (2016).
19. A. Robert, S. Funk, A. J. Kucharski, The measles crisis in Europe—The need for a joined-up approach. *Lancet* **393**, 2033 (2019).
20. World Health Organization, "Vaccines and biologicals data, statistics and graphics" (Tech. Rep., World Health Organization, Geneva, Switzerland, 2018).
21. World Health Organization, "Syria cVDPV2 outbreak situation report" (Tech. Rep. 33, World Health Organization, Geneva, Switzerland, 2018).
22. Government of the Syrian Arab Republic/World Health Organization, "Syria: EWARS Weekly Bulletin, week no. 50" (Tech. Rep., World Health Organization, Geneva, Switzerland, 2018).
23. Ö. Ergönül *et al.*, Profiling infectious diseases in Turkey after the influx of 3.5 million Syrian refugees. *Clin. Microbiol. Infect.* **26**, 307–312 (2020).
24. World Health Organization, "WHO vaccine-preventable diseases: Monitoring system. 2019 global summary" (Tech. Rep., World Health Organization, Geneva, Switzerland, 2019).
25. E. Simons *et al.*, Assessment of the 2010 global measles mortality reduction goal: Results from a model of surveillance data. *Lancet* **379**, 2173–2178 (2012).
26. M. Muscat *et al.*, The state of measles and rubella in the WHO European region, 2013. *Clin. Microbiol. Infect.* **20**, 12–18 (2014).
27. World Health Organization, "Immunization, vaccines and biologicals: Measles and rubella surveillance data" (Tech. Rep., World Health Organization, Geneva, Switzerland).
28. A. A. Salah *et al.*, "Introduction to the data for refugees challenge on mobility of Syrian refugees in Turkey" in *Guide To Mobile Data Analytics in Refugee Scenarios*, A. A. Salah, A. Pentland, B. Lepri, E. Letouze, Eds. (Springer International Publishing, Cham, Switzerland, 2019), pp. 3–27.
29. A. Lima, M. De Domenico, V. Pejovic, M. Musolesi, Disease containment strategies based on mobility and information dissemination. *Sci. Rep.* **5**, 10650 (2015).
30. J. T. Matamalas, M. De Domenico, A. Arenas, Assessing reliable human mobility patterns from higher order memory in mobile communications. *J. R. Soc. Interface* **13**, 20160203 (2016).
31. M. De Domenico *et al.*, Mathematical formulation of multilayer networks. *Phys. Rev. X* **3**, 041022 (2013).
32. M. Kivelä *et al.*, Multilayer networks. *J. Complex Netw.* **2**, 203–271 (2014).
33. M. De Domenico, C. Granell, M. A. Porter, A. Arenas, The physics of spreading processes in multilayer networks. *Nat. Phys.* **12**, 901–906 (2016).
34. US Agency for International Development, The DHS Program Demographic and Health Surveys: Available datasets. https://dhsprogram.com/data/available-datasets.cfm. Accessed 6 November 2020.
35. S. Merler, M. Ajelli, Deciphering the relative weights of demographic transition and vaccination in the decrease of measles incidence in Italy. *Proc. Biol. Sci.* **281**, 20132676 (2014).
36. F. Trentini, P. Poletti, S. Merler, A. Melegaro, Measles immunity gaps and the progress toward elimination: A multi-country modeling analysis. *Lancet Infect. Dis.* **17**, 1089–1097 (2017).
37. S. Li *et al.*, Demographic transition and the dynamics of measles in six provinces in China: A modeling study. *PLoS Med.* **14**, e1002255 (2017).
38. R. F. Grais *et al.*, Estimating transmission intensity for a measles epidemic in Niamey, Niger: Lessons for intervention. *Trans. R. Soc. Trop. Med. Hyg.* **100**, 867–873 (2006)
39. J. Lessler, W. Moss, S. Lowther, D. Cummings, Maintaining high rates of measles immunization in Africa. *Epidemiol. Infect.* **139**, 1039–1049 (2011).
40. P. Poletti *et al.*, The hidden burden of measles in Ethiopia: How distance to hospital shapes the disease mortality rate. *BMC Med.* **16**, 177 (2018).
41. V. Marziano *et al.*, Parental vaccination to reduce measles immunity gaps in Italy. *eLife* **8**, e44942 (2019).
42. Directorate General of Migration Management, "Distribution by age and gender of registered Syrian refugees" (Tech. Rep., Directorate General of Migration Management, Ankara, Turkey, 2018).
43. A. Jablonka *et al.*, Measles, rubella and varicella IgG seroprevalence in a large refugee cohort in Germany in 2015: A cross-sectional study. *Infect. Dis. Ther.* **6**, 487–496 (2017).
44. F. Trentini, P. Poletti, A. Melegaro, S. Merler, The introduction of 'no jab, no school' policy and the refinement of measles immunization strategies in high-income countries. *BMC Med.* **17**, 86 (2019).
45. H. d'Albis, E. Boubtane, D. Coulibaly, Macroeconomic evidence suggests that asylum seekers are not a "burden" for western European countries. *Sci. Adv.* **4**, eaaq0883 (2018).
46. C. Ergun, H. Gül, Urban regeneration and social segregation: The case of Istanbul. *Toplum ve Demokrasi Dergisi* **5**, 155–172 (2014).
47. B. Balkan, E. Tok, H Torun, S. Tumen, "Immigration, housing rents, and residential segregation: Evidence from Syrian refugees in Turkey" (IZA Discussion Paper 11611, IZA Institute of Labor Economics, Bonn, Germany, 2018).
48. P. E. Fine, Herd Immunity: History, theory, practice. *Epidemiol. Rev.* **15**, 265–302 (1993).
49. Organisation for Economic Co-Operation and Development, "Making integration work: Refugees and others in need of protection" (Tech. Rep., Organisation for Economic Co-operation and Development, Paris, France, 2016).
50. B. Grenfell, R. Anderson, The estimation of age-related rates of infection from case notifications and serological data. *Epidemiol. Infect.* **95**, 419–436 (1985).
51. M. J. Ferrari, A. Djibo, R. Grais, B. Grenfell, O. Bjørnstad, Episodic outbreaks bias estimates of age-specific force of infection: A corrected method using measles as an example. *Epidemiol. Infect.* **138**, 108–116 (2010).
52. J. M. Read *et al.*, Social mixing patterns in rural and urban areas of southern China. *Proc. Biol. Sci.* **281**, 20140268 (2014).
53. A. Melegaro *et al.*, Social contact structures and time use patterns in the Manicaland province of Zimbabwe. *PloS One* **12**, e0170459 (2017).
54. J. Mossong *et al.*, Social contacts and mixing patterns relevant to the spread of infectious diseases. *PLoS Med.* **5**, e74 (2008).
55. M. A. Vink, M. C. J. Bootsma, J. Wallinga, Serial intervals of respiratory infectious diseases: A systematic review and analysis. *Am. J. Epidemiol.* **180**, 865–875 (2014).
56. R. M. Anderson, R. May, *Infectious Diseases of Humans: Dynamics and Control* (Oxford University Press, Oxford, UK, 1992).
57. N. M. Ferguson *et al.*, Strategies for mitigating an influenza pandemic. *Nature* **442**, 448–452 (2006).
58. V. Colizza, A. Barrat, M. Barthélemy, A. Vespignani, The role of the airline transportation network in the prediction and predictability of global epidemics. *Proc. Natl. Acad. Sci. U.S.A.* **103**, 2015–2020 (2006).
59. S. Merler, M. Ajelli, The role of population heterogeneity and human mobility in the spread of pandemic influenza. *Proc. Biol. Sci.* **277**, 557–565 (2010).
60. S. Merler, M. Ajelli, A. Pugliese, N. M. Ferguson, Determinants of the spatiotemporal dynamics of the 2009 H1N1 pandemic in Europe: Implications for real-time modeling. *PLoS Comput. Biol.* **7**, e1002205 (2011).
61. J. Gómez-Gardeñes, D. Soriano-Paños, A. Arenas, Critical regimes driven by recurrent mobility patterns of reaction–diffusion processes in networks. *Nat. Phys.* **14**, 391–395 (2018).
62. Bosetti *et al.*, "Data repository for 'Heterogeneity in social and epidemiological factors determines the risk of measles outbreaks.'" Zenodo. https://zenodo.org/record/4227667. Deposited 3 November 2020.